OPTIMAL MANOEUVRING BETWEEN QUASI-PERIODIC ORBITS

Marcel Duering[(1)], Massimiliano Vasile[(2)], and Markus Landgraf[(3)]
[(1)(2)] *University of Strathclyde, 75 Montrose Street, G1 1XJ Glasgow, United Kingdom, t:+44(0)1415482083, {marcel.duering, massimiliano.vasile}@strath.ac.uk*
[(3)] *European Space Agency, ESOC, 64293 Darmstadt, Germany, markus.landgraf@esa.int*

Abstract: *In the past halo orbits were used for most of the spacecraft missions going to the Lagrange point regions. However, other natural motions exist near these points presenting some advantages compared to halos. Quasi-periodic motions on invariant tori are associated with frequencies and amplitudes and surround the halo and vertical Lyapunov orbits. In this paper main characteristics of quasi-periodic orbits around the far-side Lagrange point in the Earth-Moon system are discussed. Optimal manoeuvres are identified to vary properties (phases, amplitudes) of an orbit. The proposed techniques utilise the stable manifold allowing for single manoeuvre transfers. The separation of spacecraft from a periodic orbit and a rendezvous scenario are discussed with respect to future missions, that have to cope with regular vehicle traffic, rendezvous and docking activities. Fuel-optimal transfers from a halo to a quasi-periodic orbit are identified in order to separate spacecraft. A second scenario assumes two spacecraft with a given phase separation on a quasi-periodic orbit. A target orbit is defined in which the spacecraft rendezvous. Parameter studies show that phase and amplitude changes strongly depend on the time when the manoeuvre is performed.*

Keywords: *quasi-periodic orbits, gateway station, traffic management, amplitudes, phases*

1. Introduction

Recent programmatic approaches for a future in-orbit infrastructure for human and robotic space exploration programmes show serious considerations of an orbital gateway station located at the far-side Lagrange point of the Earth-Moon system (EML2), providing a flexible platform for future science and exploration missions. The Space Launch System succeeding the Space Shuttle together with the Multi-Purpose Crew Vehicle is providing the crew transportation and exploration infrastructure, and concepts are required for crew and cargo access and storing beyond Earth orbit in conjunction with payloads delivery. A gateway station at L_2 provides Moon surface access and could serve as a fuel storage and transportation system for interplanetary missions [3].

A variety of (quasi-)periodic trajectories exist in the vicinity of EML2, that can serve as nominal orbit for such a gateway station. The Lagrange point regions are particularly suitable for missions that rely on regular manoeuvres, as a high Δv is required for the transfer, but once arrived all other Δv requirements are relatively small. Manoeuvring spacecraft between different orbits become a key element for such a mission to cope with regular in-space operations, rendezvous, docking activities. The utilisation of quasi-periodic orbits increases the flexibility in planning future missions. The complexity of long-term space missions would decrease, when long stay times and any time access are driving requirements for human exploration missions. For example, new launch opportunities arise if multiple phasing options exist, or if multiple spacecraft will be launched on the same rocket and then separated in the proximity of the Lagrange point.

Section 2 gives insight into the existence of quasi-orbits and their range in frequencies and amplitudes around the far-side Lagrange point in the Earth-Moon system. It is followed by the description of optimal manoeuvres derived analytically from the linearised Lissajous motion in section 3. The knowledge from previous sections is used in the last section to identify optimal manoeuvres to change properties (phases, amplitudes) of an orbit. Manoeuvre concepts are provided to appropriately phase spacecraft on a quasi-periodic orbit, and manoeuvre between a variety of periodic and quasi-periodic orbits, including formation deployment and rendezvous scenarios.

2. Periodic and quasi-periodic orbits in the Lagrange point regions

The model used for computations is the circular restricted three-body problem (CR3BP) that describes a particle moving under the gravitational forces of a primary and a secondary body. A first assumption is that the particle is massless and the second one that the secondary body travels around the primary body in a circular orbit. The second order differential equation of motion is introduced as

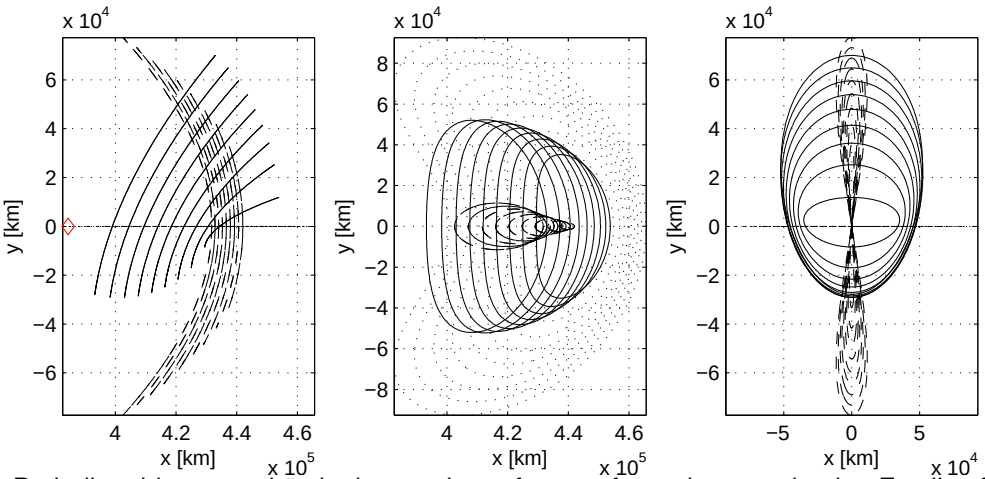

Figure 1: Periodic orbits around L_2 in the rotating reference frame in natural units. Family of Northern halo orbits (solid), vertical (dashed) and horizontal (dotted) Lyapunov orbits.

$$\begin{aligned}
\frac{d^2x}{dt^2} - 2\frac{dy}{dt} &= x - \frac{1-\mu}{r_1^3}(x+\mu) - \frac{\mu}{r_2^3}(x+\mu-1) \\
\frac{d^2y}{dt^2} + 2\frac{dx}{dt} &= y - \frac{1-\mu}{r_1^3}y - \frac{\mu}{r_2^3}y \\
\frac{d^2z}{dt^2} &= \frac{\mu-1}{r_1^3}z - \frac{\mu}{r_2^3}z
\end{aligned} \tag{1}$$

where $r_1^2 = (x-\mu)^2 + y^2 + z^2$ represents the distance from the spacecraft to the larger primary, and $r_2^2 = (x+1-\mu)^2 + y^2 + z^2$ to the smaller one. This study focuses on the Earth/Moon three-body problem assuming a mass ratio of $\mu = 0.0123$. The motion of the spacecraft is described in terms of dimensionless rotating coordinates relative to the barycentre of the system primaries. A so-called non-inertial synodic reference frame is introduced with a rotating x-axis directed from the primary to the secondary body. The two primaries are stationary in this frame, and the origin of the reference frame rotates with a constant angular velocity about the barycentre at the same rotation rate as the secondary body rotates around the primary [1]. The above introduced coordinate system is normalised such that the gravitational parameter G equals one. The non-dimensional scaling parameters for time, mass and length quantities are: t^* (inverse of the mean motion), l^* (distance between the primaries), m^* (total mass of the system). Despite the non-dimensional coordinates introduced above, the plots in this paper refer to natural units (km, s, kg).

The CR3BP possess five equilibrium points named ($L_1 - L_5$), which are also called Lagrange or libration points. L_1 and L_2 are the closest points to the secondary body. A known integral of motion in the circular restricted three body problem is the Jacobi constant C, which is used later to classify periodic and quasi-periodic trajectories. It is defined as

$$C = x^2 + y^2 + 2\frac{1-\mu}{r_1} + 2\frac{\mu}{r_2} - (\dot{x}^2 + \dot{y}^2 + \dot{z}^2). \tag{2}$$

A variety of bounded orbits and trajectories that exponentially escape or approach the neighbourhood of a Lagrange point exist. The bounded orbits are associated with the four-dimensional centre manifold. Planar and vertical Lyapunov periodic orbits have a single frequency ω_v and ω_v, respectively. Two families of halo orbits exist, which are symmetric with respect to the xz-plane. The Northern class of halo orbits is characterised with a dominant part of the motion above the z-plane. The three types of periodic orbits near the L_2 Earth/Moon Lagrange point are plotted in Fig. 1 over the Jacobian constant in a range of $C = \{3.038$ to $3.149\}$. The arrows indicate the order of the orbits by an increasing C. The circle indicates the position of the Earth, the cross Lagrange point L_2. The corresponding frequencies vary for the halo

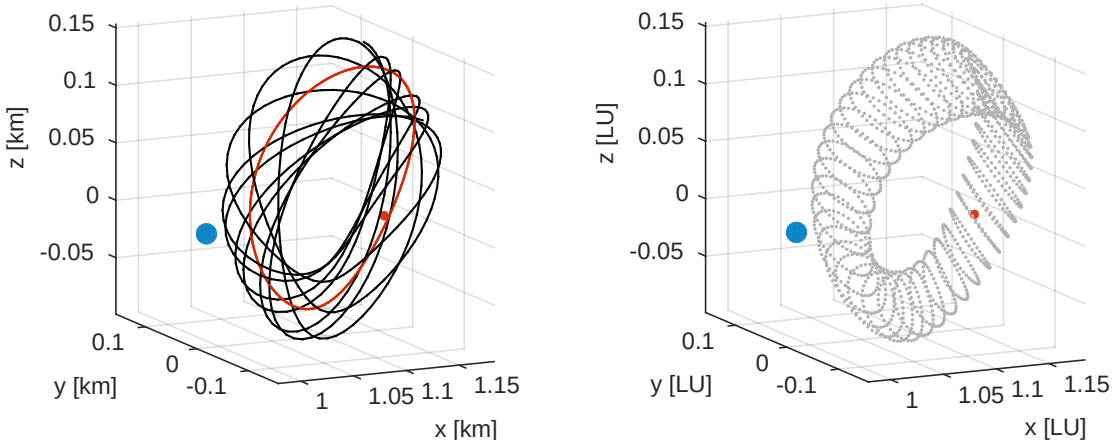

(a) (b)

Figure 2: Quasi-periodic orbit around halo orbit (left). Cross section A for a variety of tori around the generating halo orbit (right).

orbits between $\omega_{hn} = \{2.1183 \text{ to } 2.1183\}$, for the vertical Lyapunov $\omega_{vl} = \{1.6017 \text{ to } 1.7657\}$, and for the horizontal ones $\omega_{hl} = \{1.5676 \text{ to } 1.8331\}$ (2π / t^*).

There are families of orbits near halo and vertical Lyapunov orbits remain on a toroidal surface that surrounds the generating orbit. In other words, periodic orbits in the Lagrange point regions are surrounded by a variety of quasi-periodic orbits. These orbits serve as periodic seeds for the calculation of families of invariant tori. The computation of periodic orbits is based on a iterative scheme with an initial seed obtained from the third-order analytical approximation. A robust method to compute quasi-periodic trajectories utilise a Fourier representation to describe an invariant curve representing the intersection of an invariant torus with a Poincaré section. The basic algorithm is described in detail in literature [4, 5], and is modified to additionally provide the parametrisation and system frequencies. By applying this method to a wide range of periodic halo orbits of the Northern L_2 family, the family of invariant tori are computed.

Two quasi-periodic orbits are shown in Fig. 2. The cross section, together with family of feasible tori is projected onto the z-plane. The family of tori for a particular periodic orbit is reduced to a single parameter, defining either the rotation number, or the cross section. The cross section A is plotted as a function of the orbit energy within the halo and vertical Lyapunov family in Fig. 2. The curves in Fig. 2 show possible geometries. The existence of tori strongly depends on the orbital energy as the extension of those curves is constraint by the horizontal Lyapunov orbit at the same energy. The motion is directly linked to the frequency base of the torus, and can be described by a particle that is longitudinally moving about the generation orbit with the frequency ω_1, while rotating with frequency ω_2. For parameter dependencies, see Fig. 3.

3. Manoeuvres in linear theory

Any quasi-periodic orbit is characterised by its time related frequencies and phases and geometric properties such as amplitudes. In the following manoeuvres are introduced to modify those properties. The idea is to change a single parameter and maintain the others. Optimal amplitude and phase changes have already been studied in literature for the linearised equation of motion about a Lagrange point, neglecting the non-linear behaviour [2]. Analytic solutions to those problems are known from the linear Lissajous motion, where optimal manoeuvres are introduced. Those are renewed in the following. The first step is to introduce linearised dynamics in the vicinity of a quasi-periodic orbit. An entire linear solution is known for orbits around the equilibrium points. A new reference frame with the same axis definition as the synodic frame introduced above with an origin at the equilibrium point of interest is used. The linearised equations of motion have the form

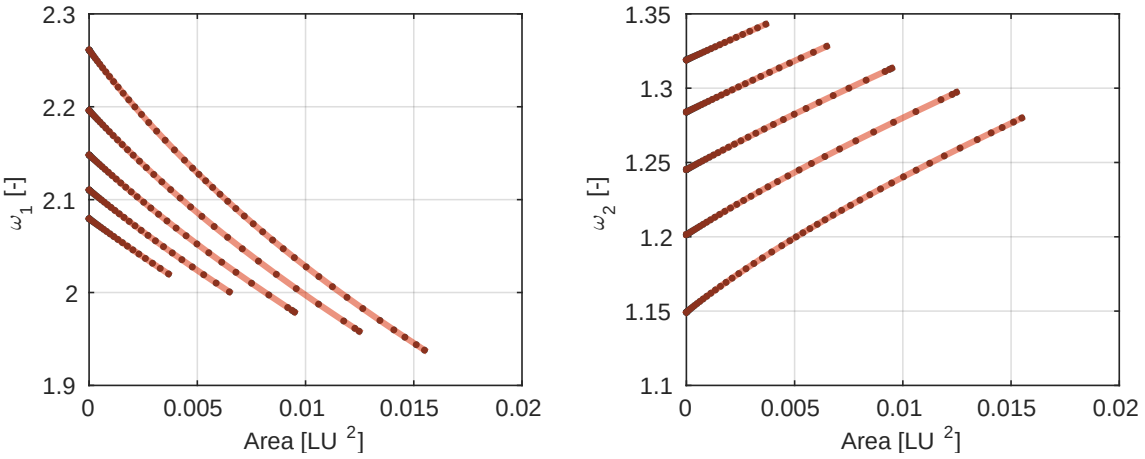

(a) (b)

Figure 3: The frequencies ω_1 (a) and ω_2 (b) plotted as a function of the continuation parameter of the torus family A for several iso-energetic quasi-periodic orbit series.

$$\begin{aligned} \ddot{x} &= 2\dot{y} + (1 + 2c_2)x \\ \ddot{y} &= -2\dot{x} + (c_2 - 1)y \\ \ddot{z} &= -c_2 z \end{aligned} \tag{3}$$

with

$$c_2 = \frac{1}{\gamma^3}(\mu + (1-\mu)\frac{\gamma^3}{(1-\gamma^3)^3} \tag{4}$$

the constant c_2 is only depended on the mass parameter and the location of the Lagrange point. Note that the expression for c_2 is only valid for the Lagrange point L_2. The linearised system is characterised by a coupled motion in the xy-plane and a decoupled one in the z-direction, as seen in Eq. 5. The in-plane phases and amplitudes relate to the motion in the xy-plane, whereas the out-of-plane parameters describe the motion in z-direction. The periodic part of the analytic solution is written with the help of an amplitude and phase as

$$\begin{aligned} x &= A_1 e^{\lambda t} + A_2 e^{-\lambda t} + A_x \cos(\omega_2 t + \theta_2) \\ y &= cA_1 e^{\lambda t} - cA_2 e^{-\lambda t} + \kappa A_x \sin(\omega_2 t + \theta_2) \\ z &= A_z \cos(\omega_1 t + \theta_1) \end{aligned} \tag{5}$$

with

$$\lambda^2 = \frac{c_2 - 2 + \sqrt{9c_2^2 - 8c_2}}{2} \qquad \omega_1^2 = c_2 \qquad \omega_2^2 = \frac{2 - c_2 + \sqrt{9c_2^2 - 8c_2}}{2} \tag{6}$$

and $c = \frac{\lambda - 1 - 2c_2}{2\lambda}$, $\kappa = \frac{\omega_2 - 1 - 2c_2}{2\omega_2}$. The equation of motion contain of an oscillatory part and hyperbolic exponential parts. The hyperbolic exponential parts comprise of a exponential part with a positive exponent, and a part with a negative exponent. The integral of motion A_1 and A_2 are related to the unstable and stable component. If A_1 is zero and a A_2 component exists, this components decays exponentially to zero. In order to avoid unstable behaviour the integral A_1 that is associated with it is set to zero.

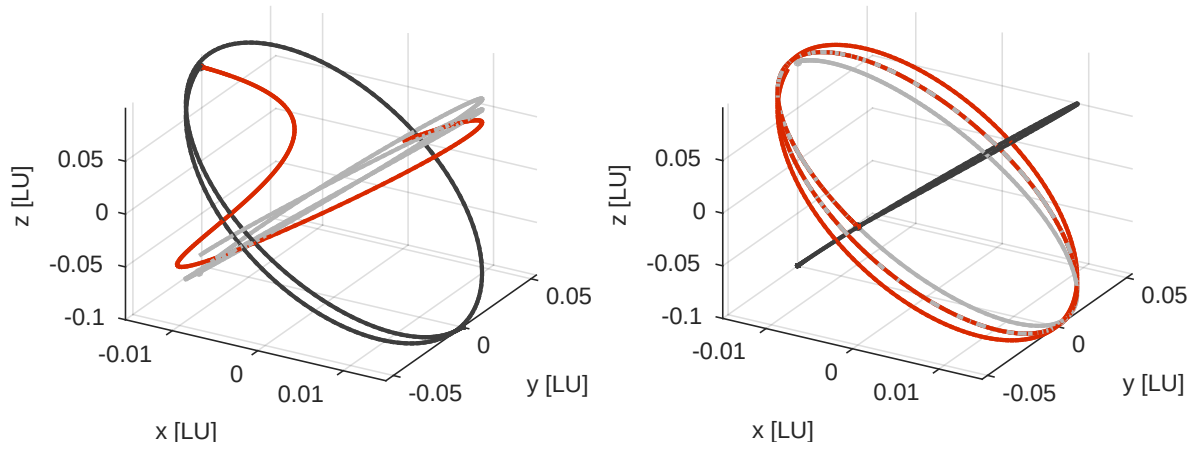

(a) (b)

Figure 4: In-plane phase change by manoeuvre conducted at time $t_m = 6.51$ days utilising stable manifold for transfer (top). Out-of-plane phase change using intersection of initial and final trajectory (bottom).

The following equation are all derived from the linear equation of motion Eq. 5. The exact derivation of the equations can be found in [2]. The manoeuvre direction is defined is such way that the unstable motion is cancelled out and the only a stable part is introduced. The manoeuvre direction and a constant β is introduced, which represents a gradient. They are given by

$$s_{dir} = \left(\frac{1}{d_1}, \frac{-\kappa}{d_2}, 0\right)^T \qquad \beta = \tan^{-1}\left(\frac{\kappa}{c}\right) \tag{7}$$

The in-plane and out-of-plane phase is analogous to the true anomaly of a keplerian orbit. They define the position of an orbiting spacecraft along the trajectory. With respect to the torus theory this implies that the spacecraft before and after the manoeuvre will be on the same torus structure. An optimal in-plane and out-of-plane phase change manoeuvre at a time t_m has the form

$$\theta_2^f - \theta_2^i = -2(\omega_2 t_m + \theta_2^i - \beta) \tag{8}$$
$$\theta_1^f - \theta_1^i = -2(\omega_1 t_m + \theta_1^i) \tag{9}$$

where the indices i correspond to initial and f to final parameters. It is required to point out that at a particular time there is only one possible jump possible with single manoeuvre strategies. Optimal solutions for amplitude changes are derived in the same way as for phase change in the previous cases. The optimal manoeuvre at time t_m to change phasing of the final orbit is of magnitude and direction

$$\Delta v_{xy} = 2A_x \sin(\omega_1 t_m + \phi_i - \beta)\|s_{dir}\| \tag{10}$$
$$\Delta v_z = 2A_z \sin(\omega_2 t_m + \psi_i) \tag{11}$$

Two transfers on a linear Lissajous orbit with a $A_z = A_x = 2 \cdot 10^4$ km are shown in Fig. 4. In both cases a linear Lissajous orbit is propagated started from $t = 0$ days, one with a phase shift of $\phi = 0$ rad (red, dashed) and $\phi = 2.946$ rad (blue, solid), which exactly correspond to the optimal shift at the manoeuvre time $t_m = 6.51$ days. The manoeuvre is executed and the satellite asymptotically reaches its new trajectory. The stable manifold of the arrival point is shown in gray, showing that the satellite uses the manifold to approach its final orbit. In this case the time until arriving at the final orbit is $\Delta t = 11.3$ days.

It is important to note that the transfers are based on a different methodology. In the in-plane case the manoeuvre does not instantly send the spacecraft onto the final orbit, but onto the stable manifold with the effect that the spacecraft asymptotically reaches its final orbit. In the out-of-plane case the position of initial and final orbit cross and with a transfer time equals zero the spacecraft continues its motion on the final orbit. multiple manoeuvres and intermediate transfer arcs may be used for more generalised cases.

4. Impulsive transfers between (quasi-)periodic orbits

Impulsive transfers between (quasi-)periodic orbits are studied with respect to an orbital gateway station. There are different options to create transfers. Two impulsive manoeuvres can be used in order to target the desired state with the first manoeuvre and the second one corrects the velocity component. The previous section provided insight into transfers that are optimal with respect to the linearised dynamics, providing a first approximation of the Δv requirement for phase changes. In the following the focus is set on single impulse transfers utilising the stable manifold in the dynamic regime of the CR3BP.

4.1. Manifold transfer optimisation

It is essential that fuel-optimal transfers are investigated for future mission relying on multiple manoeuvres once arrived at EML2. The transfers will provide flexible phasing opportunities along with the required costs. Manifold transfers are good and suitable options to manoeuvre on quasi-periodic trajectories. Those transfers are constructed by matching the outgoing manifold of the final orbit with the initial state. The advantage of a manifold transfer is that a second insertion manoeuvre is not required as the spacecraft asymptotically reaches its target. This methods offers lower Δv expenses for the transfer compared to two impulse transfer arcs. The target quasi-periodic trajectory is described by angular coordinates and the torus function. This enables to use θ_1 and θ_2 as optimisation variables without numerical integration of the final trajectory. The prime constraint is to match the initial position variables with the manifold arc.

The optimisation is initialised by scanning the positive and negative branch of the stable manifold and evaluating the closest approach to the initial state x_0, along with the costs Δv_1 to correct the velocity between the initial state and the manifold branch. An additional constraint is required if the initial position is part of the torus structure as the scan will exactly find this point as closest solution. To avoid this in the guess generation additional to the distance evaluation, the direction of the manoeuvre Δv is examined. The guess is dropped, if the second manoeuvre is along the original velocity direction.

The stable manifold is created by backward integration of a state on the quasi-periodic orbit. One manifold branch approaches the Moon, whereas the second one leaving the Lagrange point region in the opposite direction, see Fig. 5 for a partial part of the manifold for a fix $\theta_1 = 0$. A small manoeuvre is executed in the direction linearised stable direction in order to force the spacecraft onto the stable manifold. The set of parameters $(\theta_1, \theta_2, t_{tf}, \Delta v_1)$ corresponding to the smallest distance between $x_f(\theta_1, \theta_2)$ and x_0 serve

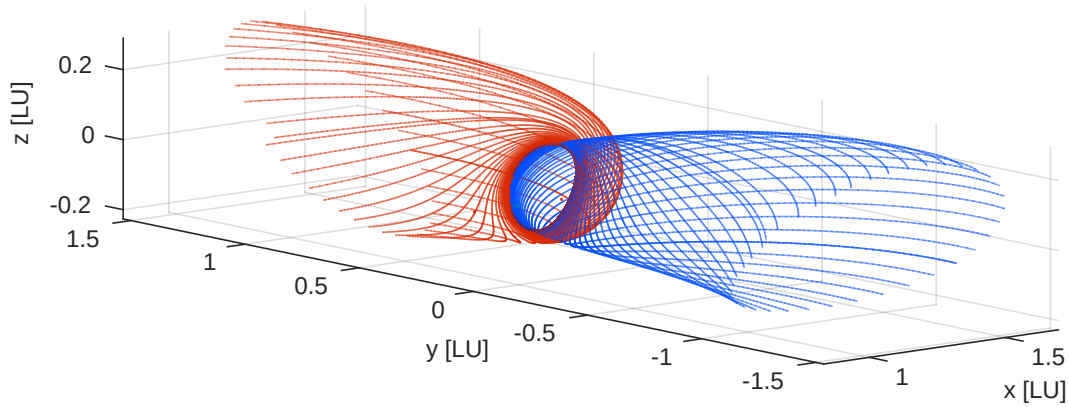

Figure 5: Partial positive and negative stable manifold branch of a quasi-periodic orbit

as initial guess in a gradient-based optimisation process. The optimisation process finally connects the stable manifold branch with the initial condition x_0. The results of the optimisation process are the position along the quasi-periodic orbit, whose stable manifold crosses the initial position. The optimal phase change is evaluated as $\Delta\theta = \theta_2 - \theta_0 - (t_m + t_{tf})\omega$ at a given time t_m.

4.2. Spacecraft separation from periodic orbit

In the following formation deployment aspects are studied. The use of a single launch vehicle to launch a set of satellites is faster and easier to realise. An efficient way has to be found to separate the satellites either during transfer or once they are inserted into orbit around the Lagrange point. Apart from such a separation scenario, transfer to nearby orbits become relevant for a gateway station concept where locations for e.g. storage are investigated. The naturally existing trajectories in the proximity of a nominal orbit provide optional operation orbits and enable an increased operational flexibility in terms of launch windows and rendezvous scenarios.

The scenario assumes two spacecraft launched and injected into a halo orbit with a orbital period of $T = 13.50$ days. The goal is to inject them into a quasi-periodic orbit in such a way that the phase difference in ω_2-direction is $120\,\mathrm{deg}$. In order to find the optimal time for such a transfer, the optimal final phases on the quasi-periodic orbit after the transfer are evaluated. Two solution are highlighted and feasible at a time t in θ_2-direction. Those present the two connection from the positive and negative branch of the stable manifold. The same effect as the linear study in the previous part. The phase θ_1 varies around zero, the small deviation from zero is caused by the different period of the initial and final orbit.

For the scenario a feasible transfer solution is highlighted in the plot. The first spacecraft is transferred at $t = 1.45$ days reaching the final quasi-periodic orbit with a phase of $\theta_2 = 0.1384$ rad after $\Delta t = 6.18$ days. At $t = 5.79$ days the second spacecraft is sent to a phase $\theta_2 = 3.9326$ rad, arriving at the final orbit in $\Delta t = 3.93$ days. The Δv for the transfer is $\Delta v_1 = 41.1\frac{m}{s}$ and $\Delta v_1 = 44.87\frac{m}{s}$. The distances between the spacecraft and relative to the halo orbit are plotted in Fig. 6.

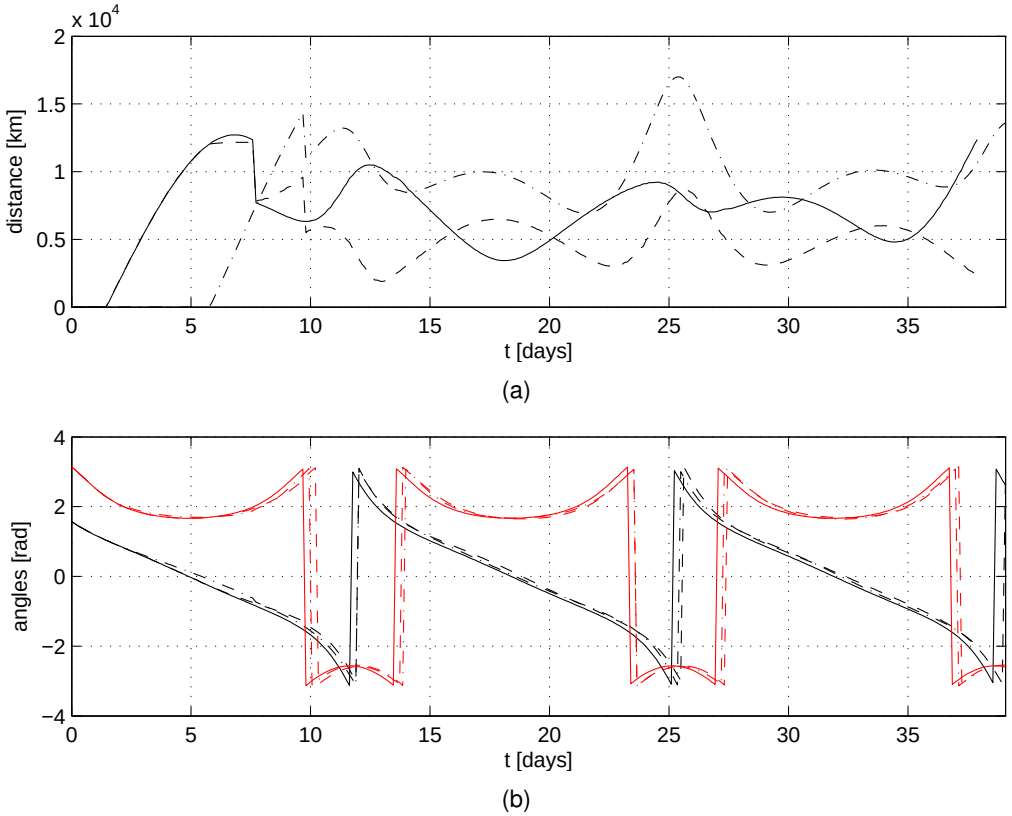

Figure 6: Geometric properties plotted as a function of time. Spacecraft are on same orbit until $t = 1.45$ days. Distance to halo orbit for first (dashed) and second (dotted) spacecraft.

4.3. In-orbit rendezvous

For a gateway traffic management it is important to reconfigure spacecraft in such a way that they rendezvous in orbit for docking activities. In past studies, phasing manoeuvres are used to fulfil mission requirements, such as for the implementation of eclipse avoidance strategies as quasi-periodic Lissajous suffer of longer eclipse periods compared with halo orbits. In contrast to the amplitude changes of the torus, phases changes maintain the geometric properties of a quasi-periodic orbit, but changes the position of a orbiting spacecraft along the trajectory. With respect to the torus theory this implies that the orbit before and after a successful transfer is described by the same torus function u.

A scenario with two spacecraft flying rendezvous manoeuvres on the same quasi-periodic orbit are studied. The quasi-periodic orbit has the following frequencies: $\omega = \{2.01, 1.40\}$. A pair of spacecraft is inserted onto the same quasi-periodic orbit with initial phases of $\theta = \{0, 0\}$ and $\theta = \{0.3137, 2.8146\}$. The objective is that both spacecraft meet at a time t at the same location. To provide a parametric analysis on phase changes along a quasi-periodic trajectory, the manifold connections are evaluated. Both spacecraft follow their nominal path until $t = 1.45$ days with an initial separation of $2.2 \cdot 10^4$ km. One spacecraft conducts a manoeuvre at $t = 1.45$ and the other one continues its nominal path. 13.55 days later both spacecraft rendezvous and follow the quasi-periodic orbit. The Δv requirement for the rendezvous is $83.38 \frac{m}{s}$. Fig. 8 shows the inter-spacecraft distance shown for a rendezvous scenario of two spacecraft (solid). Rendezvous takes place at $t = 15$ days. Distance to periodic orbit for first (solid line) and second (dashed) spacecraft.

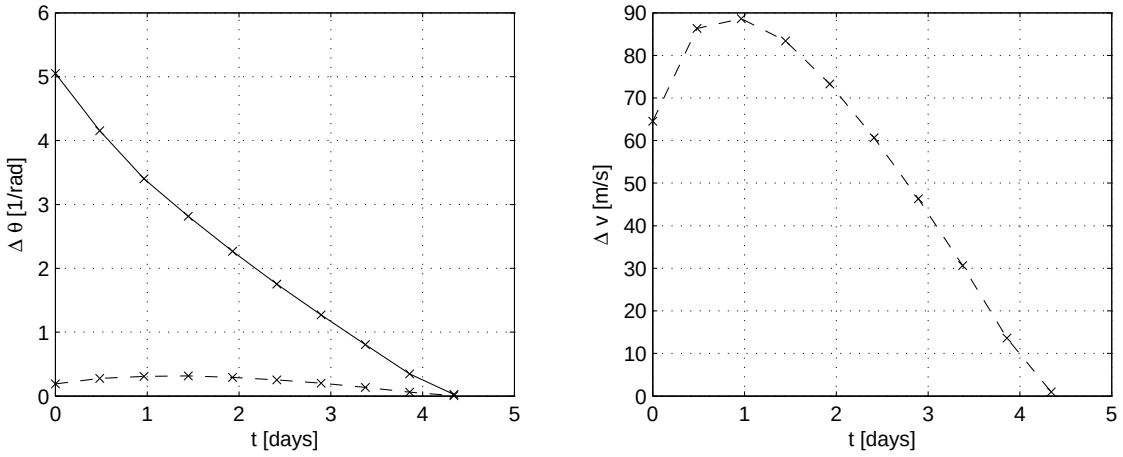

(a) (b)

Figure 7: Results of a parametric study of transfer options on a quasi-periodic orbit ($\omega_1 = 2.01$ and $\omega_2 = 1.40$).

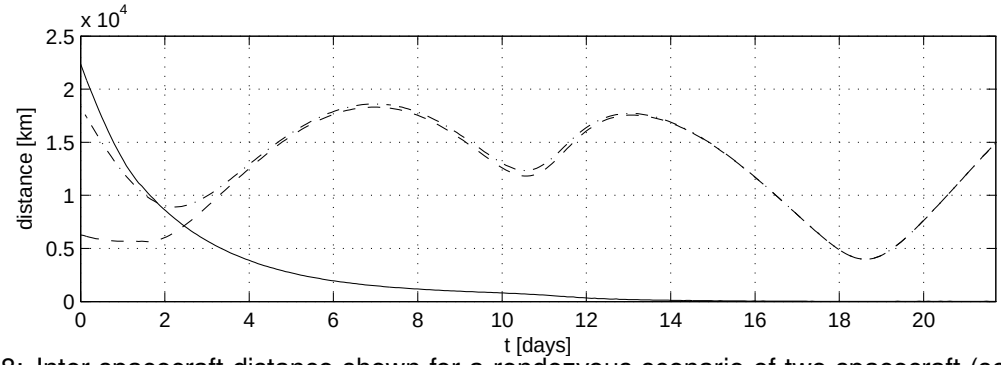

Figure 8: Inter-spacecraft distance shown for a rendezvous scenario of two spacecraft (solid). Rendezvous takes place at $t = 15$ days. Distance to periodic orbit for first (solid line) and second (dashed) spacecraft.

5. Conclusions

The exploitation of natural motion relative trajectories for traffic management around a gateway station at the far-side Earth-Moon Lagrange point allows to improve the sustainability of associated exploration scenarios. This is achieved by minimizing Δv, transfer times, and a optimum design of manoeuvre strategies. The transfers studied in this paper utilise the information on frequencies and amplitudes from existing orbits around EML2. Spacecraft separation and rendezvous scenarios prove the concept and show the flexibility in introducing regular manoeuvres to phase spacecraft along orbits that remain on a toroidal surface surrounding periodic orbits.

Acknowledgements

This work is partially funded through an ESA Networking Partnership Initiative between the University of Strathclyde and the ESA European Space Operations Centre.

6. References

[1] B.T. Barden and Kathleen C. Howell. Fundamental motions near collinear libration points and their transitions. *Journal of the Astronautical Sciences*, 46(4):361–378, 1998.

[2] Elisabet Canalias. Contributions to Libration Orbit Mission Design using Hyperbolic Invariant Manifolds. 2007.

[3] Keric Hill and Jeffrey Parker. A lunar L2 navigation, communication, and gravity mission. *AIAA/AAS Astrodynamics Specialist Conference*, (August), 2006.

[4] Egemen Kolemen, N. Jeremy Kasdin, and Pini Gurfil. Multiple Poincaré sections method for finding the quasiperiodic orbits of the restricted three body problem. *Celestial Mechanics and Dynamical Astronomy*, October 2011.

[5] Zubin P. Olikara and Daniel J Scheeres. Numerical method for computing quasi-periodic orbits and their stability in the restricted three-body problem. pages 1–20.